Electrochimica Acta 170 (2015) 131–139

Contents lists available at ScienceDirect

Electrochimica Acta

journal homepage: www.elsevier.com/locate/electacta

Electrochemical in situ FTIR spectroscopy studies directly extracellular electron transfer of *Shewanella oneidensis* MR-1

Le-Xing You [a], Lu Rao [a], Xiao-Chun Tian [a], Ran-Ran Wu [b], Xuee Wu [a], Feng Zhao [b,*], Yan-Xia Jiang [a,*], Shi-Gang Sun [a]

[a] State Key Laboratory of Physical Chemistry of Solid Surfaces, Department of Chemistry, College of Chemistry and Chemical Engineering, Xiamen University, Xiamen 361005, Fujian Province, PR China
[b] Key Laboratory of Urban Pollutant Conversion, Institute of Urban Environment, Chinese Academy of Sciences, Xiamen 361021, Fujian Province, PR China

ARTICLE INFO

Article history:
Received 11 March 2015
Received in revised form 24 April 2015
Accepted 24 April 2015
Available online 27 April 2015

Keywords:
S. oneidensis MR-1
electrochemical in situ FTIR spectroscopy
extracellular electron transfer
mutant
carbon dioxide

ABSTRACT

Cyclic voltammetry (CV) and electrochemical in situ FTIR spectroscopy (in situ FTIRS) were used to investigate the directly extracellular electron transfer (EET) of *Shewanella oneidensis* MR-1 wild type and △*omcA*-△*mtrC* mutant in this work. The CV results illustrate that the mutant still possesses electron transfer capability, but much weaker than the wild type does. In this in situ FTIRS study, some new IR bands ascribing to OmcA-MtrC protein and CO_2 were firstly collected. The EET process can be evaluated through monitoring the intensity of these bands. In water solution, the wild type has a band at 1742 cm^{-1} of $\nu_{(C=O)}$ while the mutant has one at 1712 cm^{-1} of $\nu_{(C=O)}$ during EET process. However, the band at 1742 cm^{-1} disappears but the band at 1712 cm^{-1} appears when wild type is in deuterated water solution; it is noteworthy that 1742 cm^{-1} can reappear after the sodium lactate was added into the solution. For △*omcA*-△*mtrC* mutant, the 1712 cm^{-1} band is present in both water and deuterated water solution. These all suggest that the band at 1742 cm^{-1} is ascribed to the OmcA-MtrC protein while the band at 1712 cm^{-1} belongs to some unknown protein. Meanwhile, we have also found that the band at 2342 cm^{-1} is contributed by CO_2 produced by the bacterial metabolism. The CO_2 band in the wild type was larger than that in the mutant whether the two bacteria were fed lactate or not, the data implied that electron transfer capability of the wild type is stronger than that of the mutant. We thus proposed that the amount of CO_2 can serve as a key index to evaluate the EET capability. Electrochemical in situ FTIRS is much stronger in quantitatively explanation why the wild type has a greater electron transfer capacity compared with the mutant; the function of OmcA-MtrC protein in EET process can be extracted during cell respiration.

1. Introduction

Shewanella oneidensis (*S. oneidensis*) MR-1, as a model bacterium for extracellular electron transfer (EET), can respire organic compounds and minerals. In this course, the bacterium transfers electrons from electron donors (i.e., lactate, glucose) to electron acceptors, while the cell own living demand is also satisfied [1]. Many researchers focus on studying the protein functions in *S. oneidensis* MR-1 as well as the interaction between the proteins and the electron acceptors, [2–7] such as Fe_2O_3, MnO_2 and electrodes [8]. How bacteria transfer electrons, a key scientific issue in bioelectrochemical systems, is under intensive research currently. It has been reported that there are two kinds of EET pathways: (1) Electrons can be indirectly transferred by electron shuttles, for example, riboflavin, a metabolite secreted from *S. oneidensis* [9,10]. (2) Electrons can be directly transferred from series proteins in the cell membrane, e.g. *c*-type cytochromes [11–14]. OmcA is an 83-kDa decaheme cytochrome with 708 amino acids while MtrC is 77-kDa decaheme cytochrome with 671 amino acids. In the directly EET pathway via series proteins (Scheme 1), OmcA-MtrC, as outermost proteins in the cell outer membrane, play a very important role in transferring electrons [4,11].

Although electron transfer in the cell is complex, a current signal is able to provide information about EET from a perspective of electrochemistry [15]. Previous works have indicated that

* Corresponding authors at: State Key Laboratory of Physical Chemistry of Solid Surfaces, Department of Chemistry, College of Chemistry and Chemical Engineering, Xiamen University, Xiamen 361005, Fujian Province, PR China.
Tel.: +86 592 2180181; fax: +86 592 2180181.
E-mail addresses: fzhao@iue.ac.cn (F. Zhao), yxjiang@xmu.edu.cn (Y.-X. Jiang).

http://dx.doi.org/10.1016/j.electacta.2015.04.139
0013-4686/

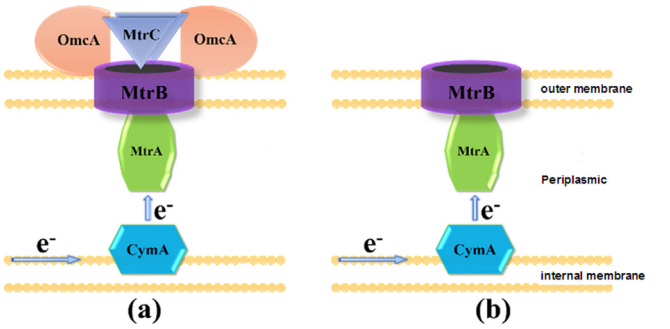

Scheme 1. *c*-type cytochromes in electron-transfer chain terminal of (a) *S. oneidensis* MR-1 wild type and (b) △*omcA*-△*mtrC* mutant [9].

S. oneidensis MR-1 shows an electrochemical activity [16,17]. Moreover, the mutant with the gene of OmcA-MtrC knocked out (see Scheme 1b) has a weak electrochemical activity [8], which indicated that △*omcA*-△*mtrC* mutant possesses some ability of transferring electrons [18]. The function of △*omcA*-△*mtrC* mutant in transferring electrons is not completely lost, therefore, it can be inferred that other proteins in the mutant are playing the role of EET [18]. Till now, it is still a deduction and needs more evidences to prove it.

For complicated cells, it is difficult to clearly state which proteins/groups are response for electron transfer processes only by cyclic voltammetry (CV) or differential pulse voltammetry (DPV). The data obtained in the CV or DPV are just the average signal of total electrochemical behavior; while more information about vibration groups can be obtained by FTIR measurements in a molecular level. Some researchers have employed FTIR spectroscopy to study *S. oneidensis* MR-1 [19–21]. Elzinga et al. used attenuated total reflection (ATR)-FTIR spectroscopy to study the influence of pH value when *S. oneidensis* was loaded on hematite sorbent and they found that the attachment mode of reactive P-groups varied with pH value [22].

Electrochemical in situ FTIRS can provide information about optical absorbance of particular species in solution or on electrode surface during the electrochemical reaction, and it can monitor the change of species at the molecular level. More information, e.g. bacterial activity and capability of electron transfer, can be extracted during cell respiration by this in situ technique. Only a few applications of electrochemical in situ FTIR in investigating the EET have been reported [23–25]. Busalmen and Feliu et al. studied the surface redox processes in *G. Sulfurreducens* by ATR-surface enhanced infrared absorption spectroscopy, and found that external cytochromes had responded to the potential of the electron acceptor. Collectively, these studies only assign several IR bands to the heme group in cytochromes *c* rather than to certain protein of *S. oneidensis* and *G. Sulfurreducens* species.

A better understanding of the EET mechanism benefits the development of various bioelectrochemical technologies, such as microbial fuel cells [26]. It also provides a further comprehension of microbial ecology [27]. Since OmcA-MtrC protein at the outmost cell membrane plays a key role in EET (i.e. the capability of transfer electrons), we thus monitor the EET process via tracking IR bands ascribing to OmcA-MtrC protein. For comparison, the mutant that was knocked-out the gene of OmcA-MtrC of *Shewanella oneidensis* MR-1 was used here to determine the IR band assignment, i.e., the difference between two strains is that membrane bonded OmcA-MtrC protein. Through comparing EET of the wild type and its mutant by investigation of CV and in situ FTIR spectroscopy, the IR bands and the function of OmcA-MtrC protein in EET process can be clearly obtained during cell respiration.

2. Experimental

2.1. Chemicals

The chemical reagents, $Na_2HPO_4{\cdot}12H_2O$, KH_2PO_4, NaCl, sodium lactate, are of analytical grade. Luria–Bertani (LB) medium used in culture was prepared with 10 g L^{-1} peptone (biological reagent), 5 g L^{-1} yeast extract (biological reagent) and 5 g L^{-1} NaCl. Phosphate buffer solution (PBS) (pH 7.0) was made by mixing 50 mM solutions of $Na_2HPO_4{\cdot}12H_2O$ and KH_2PO_4. All aqueous solutions were prepared with ultrapure water (resistivity > 18 MΩ cm) purified by a Milli-Q Labo apparatus (Nihon Millipore Ltd). Deuterated water (D_2O, Sigma-Aldrich chemistry) is 99.99% high-purity.

2.2. Cell cultivation and prepared

The 100 mL of LB medium prepared with 50 mM PBS was sterilized at 121 °C for 20 min before the bacterium were cultured [28]. Then the *S. oneidensis* MR-1 wild type and the mutant were cultured aerobically in a constant temperature incubator with slight shaking (120 rpm) at 30 °C for 25 h [28]. The optical density at 600 nm (OD_{600}) was about 1.0 at that time. Subsequently, the cell culture was centrifuged at 8000 rpm for 5 min and rinsed with doubly distilled water twice to reduce the riboflavin function on mediated EET.

2.3. Cyclic voltammetric experiments

In all electrochemical experiments, saturated calomel electrode (SCE) was used as the reference electrode, and Pt foil served as counter electrode. The working electrode employed here was Au polycrystalline disk. Before each experiment, the working electrode was successively polished in 1, 0.5 and 0.03 μm aluminum oxide powder then was rinsed with ultrapure water repeatedly. The cleanliness of the bare electrode surface was checked by cyclic voltammetry in 0.5 M H_2SO_4 solution (Electronic Supplementary Information (ESI) Fig. 1) [29].

5 μL cells collected in section 2.2 was delivered to the surface of clean Au electrode. Up to now, it is still difficult to get a monolayer

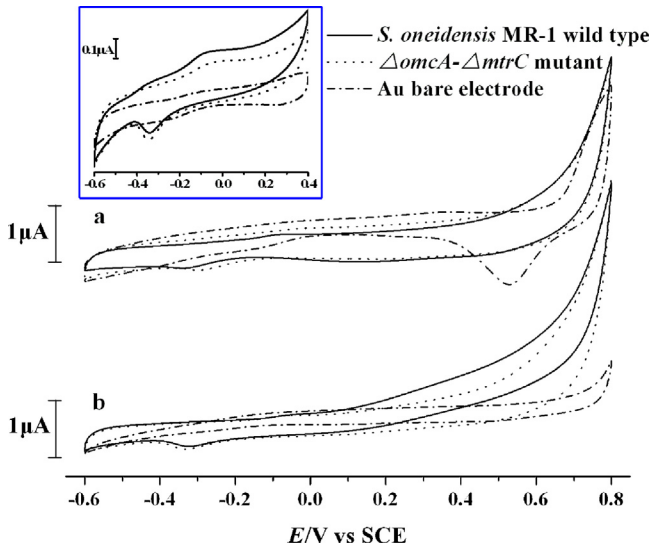

Fig. 1. Cyclic voltammograms in 50 mM PBS (a) and 50 mM PBS + 10 mM sodium lactate (b), at an Au polycrystalline electrode (dashed dot line), *S. oneidensis* MR-1 wild type modified Au electrode (solid line), and △*omcA*-△*mtrC* mutant loaded Au electrode (dot line) at pH 7; and the inset is enlarged drawing of Fig. 1 (a) with upper limit potential of 0.4 V; sweep rates: 10 mV s^{-1}.

during the biofilm development on electrode surface. The bacterium loaded Au electrode was then used in electrochemical and spectroscopic experiments. The cyclic voltammetric experiments (CHI 660D, Shanghai Chenhua Instruments Co., Ltd.) were performed to study the intrinsic electrochemical properties of cells. Oxygen was removed from the solution by bubbling N_2 before for 10 min in each experiment and this atmosphere was maintained by a flow of N_2 during the whole experiments. All the experiments were carried out at room temperature.

2.4. Electrochemical in situ FTIR experiments

Bacteria will lost their activity during dry process, while the cells keep their activity in water solution. In order to compare the difference between the alive cells and the dead ones, electrochemical in situ FTIR spectra for the cells in water solution and transmission FTIR spectra for bacteria dried on CaF_2 window were respectively collected.

In the electrochemical in situ FTIR spectra, reference potential (E_R) is set at -0.50 V and sample potentials (E_S) are set at the potentials of bacteria performing respiration. The resulting spectrum was presented as the relative change in reflectivity that is calculated as follows.

$$\frac{\Delta R}{R} = \frac{R(E_S) - R(E_R)}{R(E_R)} \quad (1)$$

Where $R(E_S)$ and $R(E_R)$ are single-beam spectra through co-added and averaged interferograms processes at E_S and E_R respectively. FTIR measurements were carried out with a Nexus 870 spectrometer (Nicolet) equipped with a liquid nitrogen-cooled MCT-A detector. A CaF_2 disk was used as IR window in the electrochemical in situ FTIR cell as previously reported [30]. Incident IR beam irradiates on the IR window, and then passes through the thin layer between the electrode and the window and further reflexes through the window into the detector (see ESI Scheme 1). An Au electrode about 5 mm in diameter covered with bacterium (as described in section 2.3) was used in FTIR measurements. A total of 400 scans using an instrumental resolution of 8 cm^{-1} were collected and averaged at each potential. Multi-stepped FTIR spectroscopic technique was applied in order to examine the change of the characteristic functional groups during the electrochemical redox processes.

S. oneidensis MR-1 wild type and △*omcA*-△*mtrC* mutant were respectively dripped onto the CaF_2 window and then dried in air to form a dry film. Pure sodium lactate (liquid) was dripped into another CaF_2 window to form a thin liquid layer. The dry film of cells and the thin liquid layer of lactate were respectively delivered to transmission spectroscopic analysis. 32 interferograms of the transmission spectrum of bacteria and sodium lactate were respectively collected in IR liquid cell, and air background was used as reference spectrum. According to the following formula

$$A(absorbance) = -log\frac{R_S}{R_R} \quad \text{and,}$$

the result spectrum is calculated as follows.

$$\%T(transmittance) = \frac{R_S}{R_R} \times 100 \quad (2)$$

Where R_S and R_R are the sample and reference spectrum collected in transmission FTIR spectroscopic detection, respectively.

In order to investigate the capability of bacterial respiration and avoid the water interference in the 1585 ~ 1700 cm^{-1} range, water was replaced by deuterated water (D_2O) (ESI section 2) [31] during the in situ FTIR investigation. Sodium lactate was dissolved in PBS deuterated water (PBS D_2O solution), and 22 interferograms of the transmission spectrum of sodium lactate PBS D_2O solution were collected in a 6 μm thick thin layer between two CaF_2 windows, referring to the spectrum of PBS D_2O solution. The result was also presented as difference spectrum calculated as formula (1), in which $R(E_S)$ and $R(E_R)$ are sample spectrum in E_S and reference spectrum in E_R respectively.

3. Results and Discussion

3.1. Cyclic voltammetry

The CVs of *S. oneidensis* MR-1 wild type, △*omcA*-△*mtrC* mutant and bare Au electrode in 50 mM PBS were shown in Fig. 1a. The increasing current on bare Au electrode in the positive-going sweep at potentials higher than 0.6 V, is corresponding to oxidation of the active species on gold surface or the chemisorption of oxygen from water [32]. The characteristic reduction peak of gold oxides is located at 0.53 V in the negative-going sweep. Due to the amount of cells on the surface of electrode cannot be precisely determined, we do not compare the current value between the wild type and the mutant in this paper. With *S. oneidensis* loaded on Au electrode, a pair of redox peaks which is corresponding to *c*-type cytochromes was observed [8]. The peak-to-peak separation ΔE_p ($\Delta E_p = E_{pa} - E_{pc}$) on CV curves can be used as a measurement of the kinetic hindrance exerted by bacterial layers on the electron transfer process. From the results in the inset of Fig. 1, the oxidation peaks of the wild type and the mutant are observed at ca. −0.05 V while the reduction peaks locate at ca. −0.35 V. Thus, the value of ΔE_p is ca. 300 mV, indicating that bacterial layers present a large barrier effect on heterogeneous electron-transfer between Au electrode and cytochromes *c* [33].

Lactate was used as an electron donor in the system which is the energy source for bacteria. When lactate is added into the solution, the change current or potential represents the response of EET process in live cells. In order to obtain a complete CV curve, the positive potential limit was extended to 0.8 V. Fig. 1b showed the CVs of *S. oneidensis* MR-1 wild type, △*omcA*-△*mtrC* mutant and bare Au electrode when lactate was added into the solution. As can be seen lactate had not been catalytically oxidized by bare Au electrode, which is shown in the dashed dot line of Fig. 1b, but it was adsorbed on bare Au surface and restrained the oxidation of bare Au electrode. The adsorptive phenomenon of lactate was found in the following electrochemical in situ FTIR experiments. The oxidative current of the bacteria loaded Au electrode increases

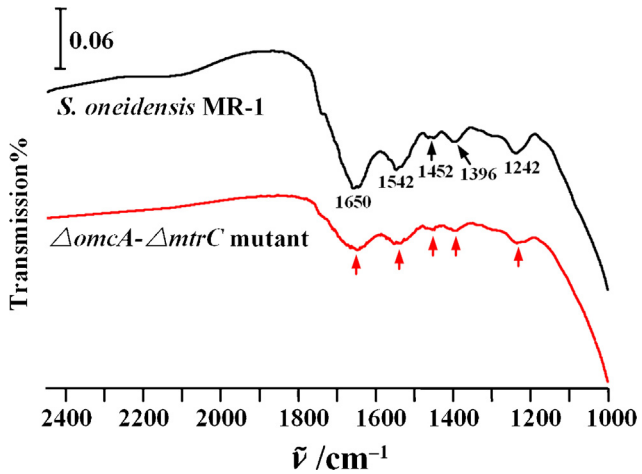

Fig. 2. The transmission infrared spectra of dry films on CaF_2 window with *S. oneidensis* MR-1 wild type and △*omcA*-△*mtrC* mutant referring to the air spectrum; 32 scans collected; resolution is 4 cm^{-1}.

Table 1
IR assignments of *S. oneidensis* cells and lactate [2,19–22,34,35].

Wavenumber(cm^{-1})	assignments
1742	$\nu_{(C=O)}$ in −COOH of OmcA-MtrC
1712	$\nu_{(C=O)}$ in −COOH for other proteins
1684	$\nu_{as(-OCO)}$ of lactate in water
~1655	amide I: $\nu_{(C=O)}$ and $\nu_{(C-N)}$ and $\delta_{(-NH)}$ in amines
1588	$\nu_{as(-OCO)}$ of lactate in D_2O
1542~1549	amide II: $\nu_{(C-N)}$ and $\delta_{(-NH)}$
1455~1461	$\delta_{as(CH_3)}$ of lactate
1450~1456	$\delta_{(CH_2/CH_3)}$ in bacteria
1418~1423	$\nu_{s(-COO)}$ of lactate
1412	$\nu_{s(-COOH)}$ in bacteria
1384/1396	$\nu_{s(-COOH)}$ in bacteria
1354	$\nu_{s(-COOH)}$ in bacteria
1235~1242	$\nu_{(C=O)}$ in $^{-}$COOH; $\nu_{(P=O)}$ in PO_4^{3-}
1150~1000	$\nu_{s(PO2)}$; $\nu_{(ring)}$; $\nu_{(C-O)}$; $\nu_{(P=O)}$; $\nu_{(C-OH,\ C-O-C)}$; $\nu_{(P-OH,\ P-OAu)}$, $\nu_{(ring)}$

by lactate adding when the potential changed from 0 to 0.8 V, indicating that both the wild type and the mutant have possessed the EET nature. The result also agrees with the literature reported by Meitl et al [16]. Moreover, the onset oxidation potential of lactate on the wild type showed 50 mV lower than that of the mutant, suggesting that the catalytic ability of the mutant was weakened when OmcA-MtrC protein was absent. These results are in accordance with the refrence [18]. Moreover, the CVs of bacteria with different scan rates are also studied in ESI Fig. 2.

3.2. The transmission infrared spectroscopy

Fig. 2 depicts the transmission infrared spectra of two dry film of *S. oneidensis* MR-1 wild type and △*omcA*-△*mtrC* mutant. The bacterial proteins are denaturated during the drying process, thus the bioactivity of bacteria would be lost. In this case, the key IR bands assigned to the proteins related to EET may not be found in the IR spectra. It can be seen that the characteristic infrared absorption of the two spectra of the wild type and its mutant are similar in Fig. 2. Five clear bands located respectively at ca. 1650, 1542, 1452, 1396 and 1242 cm^{-1} in range from 1800 to 1100 cm^{-1}. The details of IR assignments of *S. oneidensis* cells are listed in Table 1 [2,19–22,34,35].

Fig. 3a shows the transmission IR spectra of the thin liquid layer of pure sodium lactate. A broad band at 1585 ~ 1700 cm^{-1} in Fig. 3a, seriously suffering from the interference of the water, is related to the asymmetric $\nu_{as(-OCO)}$ stretching vibration in pure sodium lactate [34]. The bands at ca. 1455, 1420 and 1085 cm^{-1} can be respectively attributed to the $\delta_{as(-CH3)}$ bending vibration, the $\nu_{s(-COO)}$ and $\nu_{(C-O)}$ stretching vibration of lactate [34]. When lactate was dissolved in PBS water solution, many bands are overlapped by the band of water, so little useful information can be obtained. In order to eliminate the effect of the water, D_2O was used here instead of H_2O. As can be seen from Fig. 3b, three bands were found at 1588, 1461 and 1085 cm^{-1}, which can be ascribed to $\nu_{as(-OCO)}$,$\delta_{as(CH3)}$ and $\nu_{s(C-O)}$ in lactate. The other bands locating at ca. 2295 and 1207 cm^{-1} can be assigned to the characteristic absorption of D_2O solvent (Table 1).

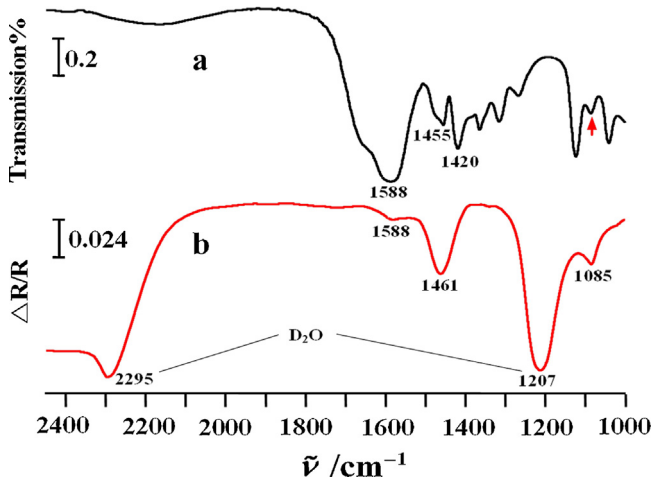

Fig. 3. (a) The transmission IR spectrum of pure sodium lactate (liquid) referring to the air IR spectrum; 32 scans collected; resolution is 4 cm^{-1}; (b) The transmission IR spectrum of sodium lactate in PBS D_2O solution referring to the lactate-free PBS D_2O IR spectrum; 22 scans collected; resolution is 8 cm^{-1}.

3.3. The electrochemical in situ FTIR spectroscopy

It can be seen from the CV in Fig. 1 that no electrochemical reaction happens at −0.5 V, which was chosen as the reference potential, $R(E_R)$, for the reference spectrum. Sample spectra $R(E_S)$ were collected with an interval of 0.1 V from −0.1 to 0.4 V in the PBS, and the potentials were extended to 0.8 V in the PBS containing lactate. The resulting data are obtained from the potential difference spectra which are calculated according to formula (1).

When the potentials were applied to the wild type or the mutant modified Au electrode in 50 mM PBS, a series of spectra were obtained in Fig. 4(a, c). Positive-going bands appeared at 1742, 1655, ~1549, 1452, ~1384, 1242 and 1098 cm^{-1} for the wild type in Fig. 4a, and occurred at 1712, 1655, ~1549, 1452, ~1396, 1242 and 1098 cm^{-1} for the mutant in Fig. 4c. It is noticed that the intensities of positive-going bands in Fig. 4(a, c) such as 1742 or 1712, 1655, ~1549, 1452, ~1396 and 1242 cm^{-1} increase with the potential when it is shifting from −0.1 to 0.4 V. The latter four bands, which are attributed to the characteristic bands of *S. oneidensis* MR-1, are consistent with the foregoing transmission spectra of Fig. 2. The band at 1655 cm^{-1} is close to the absorptive position of water, hence it is difficult to know if it is from the characteristic bands of the bacterium. And the bands between 1150 and 1000 cm^{-1} are complex and overlapped by the stretching vibrations of C–O and P–O, therefore, they are also difficult to be assigned (shown in Table 1) [20].

Compared the spectra of Fig. 4a and Fig. 4c, there was an obvious difference between the wild type and the mutant is that the wild type has a band at 1742 cm^{-1} (Fig. 4a), while the mutant has one at 1712 cm^{-1} (Fig. 4c) during their EET process. The both bands at 1742 and 1712 cm^{-1} were assigned to the stretching vibration of carbonyl $\nu_{(C=O)}$. However, the two bands at 1742 or 1712 cm^{-1} are not observed in the dry film of the wild type and the mutant in Fig. 2. Wang *et al* [35]. reported that no carbonyl band

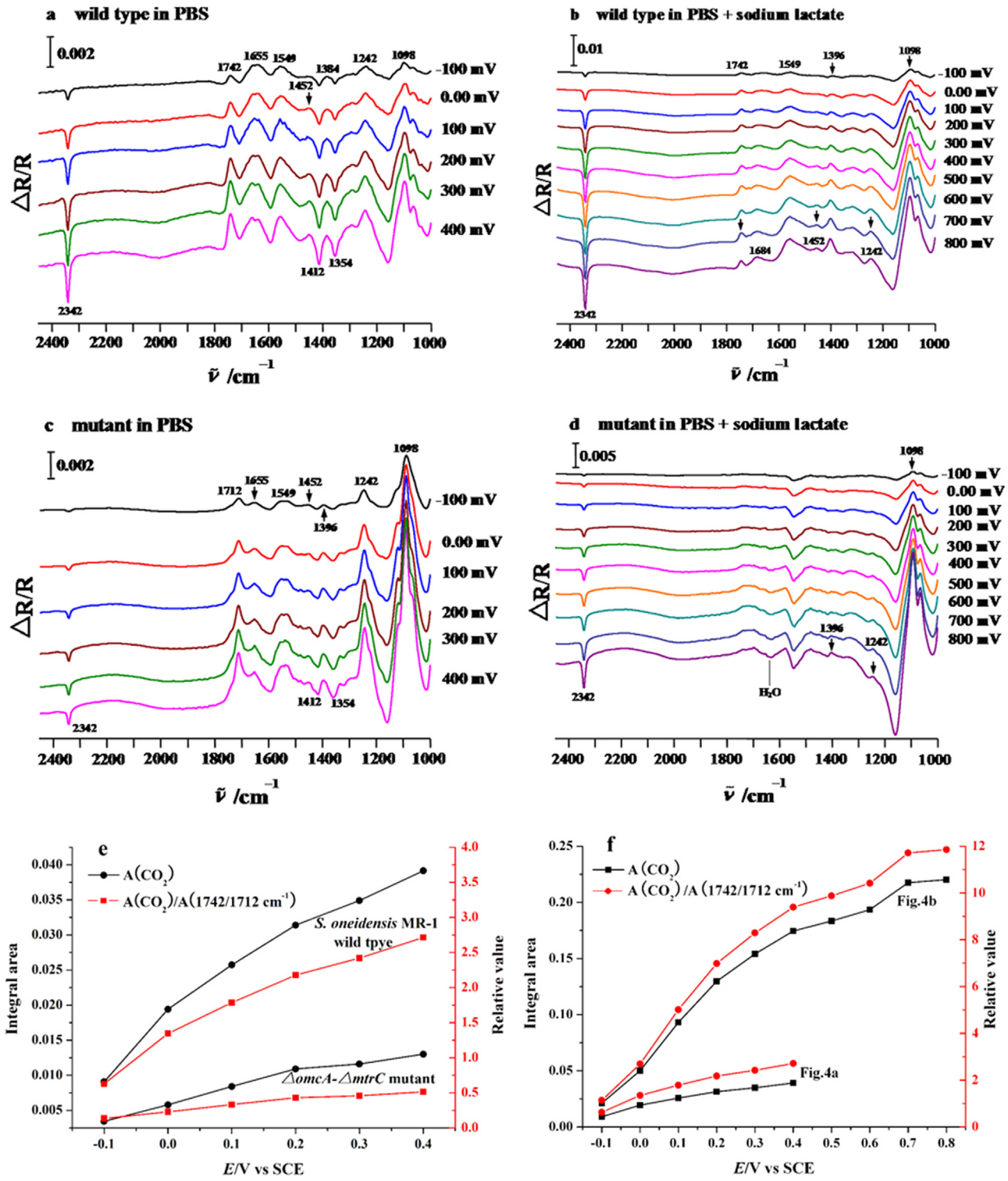

Fig. 4. Electrochemical in situ FTIR spectra in 50 mM PBS (a and c) and 50 mM PBS + 10 mM sodium lactate (b and d), at a *S. oneidensis* MR-1 wild type modified Au electrode (a and b), and △*omcA*-△*mtrC* mutant loaded Au electrode (c and d); ER is −0.5 V, E_S is indicated in every spectrum, 400 scans collected; resolution is 8 cm^{-1}; (e) The absolutely integral intensity of CO_2 IR band and the relative value of I_{CO2} / $I_{C=O(at\ 1742\ or\ 1712\ cm\text{-}1)}$ calculated from (a,c) for two bacteria respectively, (f) *S. oneidensis* MR-1 wild type from (a, b) before and after adding the lactate (b).

(1850 ∼ 1650 cm^{-1}) was found in cells after being dried at 60 °C for 10 min. Parikh *et al* [20]. also reported that an EET process happens when *S. oneidensis* is mixed with colloidal α-Fe_2O_3, and the carbonyl band at 1720 cm^{-1} was observed. Therefore it can be inferred that the bands at 1742 and 1712 cm^{-1} were the characteristic absorption bands in the wild type and the mutant involved in EET process. The speculation can be mutual corroboration by the transmission infrared spectra of dead cells in two dry films (Fig. 2). In addition, the two negative-going bands at ca. 1412 and 1354 cm^{-1} can be attributed to the $\nu_{s(-OCO)}$ stretching

vibration of protonated carboxyl groups which are the oxidation products of redox proteins. A sharp negative-going band around at ca. 2342 cm^{-1} corresponding to the O–C–O asymmetric stretching mode of CO_2 occurs and increases with potentials. It is ascribed to the product of metabolism of cells at elevated potentials.

When lactate was added into the PBS solution and then the spectra changed, which is shown in Fig. 4(b, d). The IR bands at 1742, ~1549, 1452, 1242 and 1098 cm^{-1} in Fig. 4b are clearly observed and showed no obvious difference with the results in Fig. 4a. Because the intensity of the CO_2 band is obviously larger than that of lactate-free solution, the intensity of CO_2 band is closely related to the amount of CO_2 produced mainly by the oxidation of lactate, we proposed that the intensity of the CO_2 IR band can be used as the benchmark to estimate the activity of bacteria.

Accordingly, we studied the relationship between the intensity of the CO_2 IR band and the applied potentials (Fig. 4e and 4f). It can be seen from the black lines, the absolute intensity of CO_2 IR band increases with the rise in potentials. However, considering the amount of cells is not precisely consistent on the surface of Au electrode, we use the relative intensity of the IR band to assess the CO_2 amount so as to decide capacity of bacterial metabolism. The intensity of C = O IR band at 1742 or 1712 cm^{-1} at −100 mV is taken as a standard to measure of the relative intensity of CO_2 in present condition. The relative intensity of CO_2 IR band was thus defined as I_{CO2} / $I_{C=O}$ (at 1742 or 1712 cm^{-1} for the wild type and the mutant respectively). From the red lines in Fig. 4e and 4f, the relative intensity of CO_2 IR band has increased with the rise of potentials and it indicates that bacterial metabolism capacity increases with the rise of potentials. It is noteworthy that the absolute and relative intensity of CO_2 band of the wild type are much higher than that of the mutant (Fig. 4e), the reason may be that electron transfer capability in the wild type is stronger than that in the mutant. In the presence of lactate, the intensity of CO_2 IR band increase even more greatly (Fig. 4b, d, f), and this illustrates that bacterial EET activity increases. The absolutely integral intensity of CO_2 IR band of wild type and mutant from Fig. 4 (b, d) was also shown in ESI Fig. 3. It shows that the intensity of CO_2 IR band is larger in the wild type than that in mutant. The conclusions were coinciding with the results of CV, but electrochemical in situ FTIRS method is more quantitative in explaining the reason why the wild type has greater electron transfer capacity compared with mutant.

As shown in Fig. 4b and 4d, a new broad positive-going band at ca. 1684 cm^{-1} appears for wild type (Fig. 4b) when lactate was added into 50 mM PBS solution, but does not occur for the mutant (Fig. 4d). This band is strongly interfered by water and it is difficult to be assigned. Most of the features observed for the proteins in bacteria are barely seen in Fig. 4d especially for the band at 1712 cm^{-1} for △*omcA*-△*mtrC* mutant. The bands ascribed to lactate are seriously interfered by the absorption of the water bending mode which makes it difficult to identify them. Therefore, H_2O was replaced by D_2O solvent to perform the IR measurement in this study.

When D_2O was served as a solvent to prepare the solution, the interference by H_2O was eliminated. As seen from Fig. 5a of the wild type, the band at 1712 cm^{-1} appears in PBS solution but not at

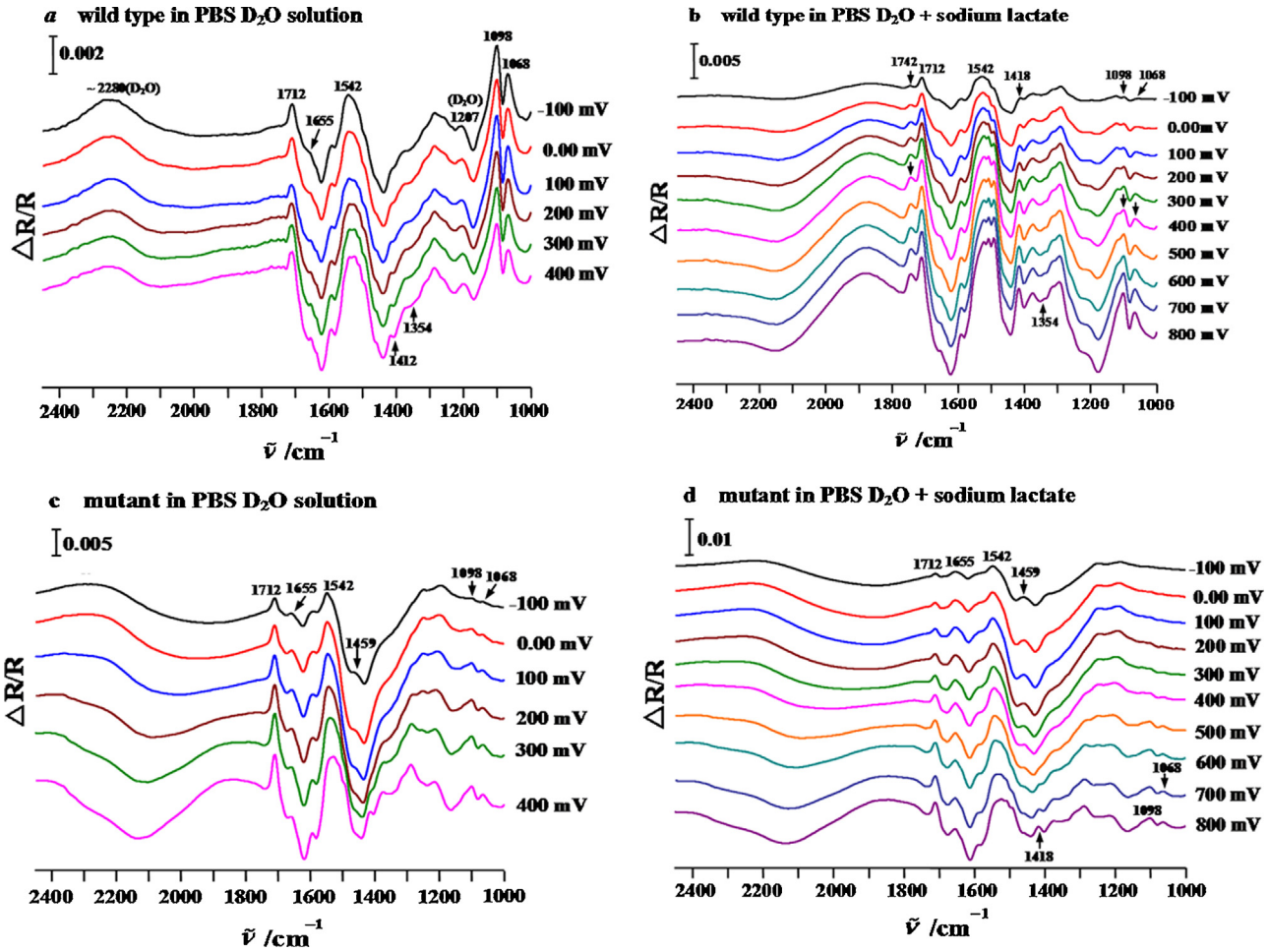

Fig. 5. Electrochemical in situ FTIR spectra in 50 mM PBS D_2O solution (a and c) and 50 mM PBS D_2O solution + 10 mM sodium lactate (b and d), at an *S. oneidensis* MR-1 wild type modified Au electrode (a and b), and △*omcA*-△*mtrC* mutant loaded Au electrode (c and d); E_R is −0.5 V, E_S is indicated in every spectrum, 400 scans collected; resolution is 8 cm^{-1}.

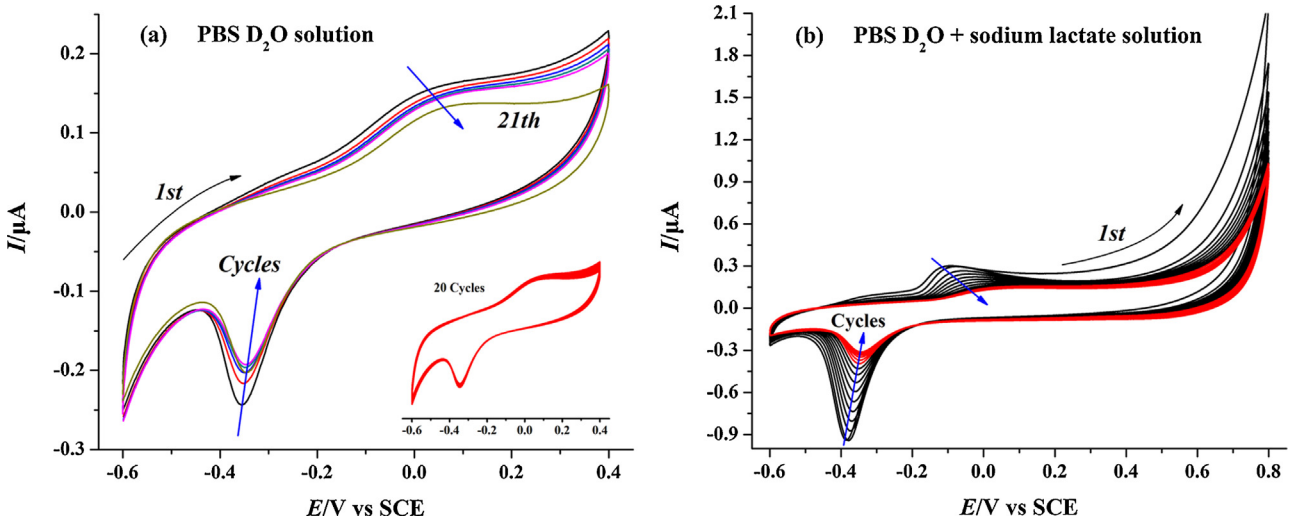

Fig. 6. The cyclic voltammograms of bare Au electrode loaded with *S. oneidensis* MR-1 wild type in 50 mM PBS D_2O solution (a) and 50 mM PBS D_2O solution containing 10 mM sodium lactate (b); Scan rates: 10 mV s^{-1}.

1742 cm^{-1}. When lactate was added to the solution, the band at 1742 cm^{-1} reappeared while the band at 1712 cm^{-1} was still present (Fig. 5b). The intensity of the band at 1742 cm^{-1} is much lower than that in water and also weaker than that at 1712 cm^{-1}. It is interesting to observe that the band of 1742 cm^{-1} is closely related to the metabolism while the bacteria is respiring lactate. Furthermore, the amide I mode of the proteins at ca. 1655 cm^{-1} and other bands, 1542, 1354, 1098 and 1068 cm^{-1}, can also be clearly found in these two spectra. However, some positive-going bands like 1452 and 1242 cm^{-1} are obscure to be observed. The band at ca. 1418 cm^{-1} attributed to $\nu_{s(-COO)}$ of lactate is also found in Fig. 5b and it increases with potential. As for △*omcA*-△*mtrC* mutant, the bands found in Fig. 5c and Fig. 5d are similar to those in Fig. 5a. The difference is that the intensity of the band at ca. 1459 cm^{-1} decreases with the increase of the potentials and then disappears. Under careful observation, we can see that the band at 1418 cm^{-1} appears at −100 mV for the wild type while it is observed at 600 mV for the mutant. This result may be related to OmcA-MtrC protein. The most noteworthy is that the band assigning to CO_2 has not been observed in D_2O solution in Fig. 5.

D_2O, in general, is cytotoxic to bacteria, it depresses the metabolism activity of cells. The cyclic voltammetry curve in D_2O solution for *S. oneidensis* MR-1 wild type was shown in Fig. 6. The bacteria prefer to adsorbing onto electrode surface rather than suspending into the toxic D_2O solution, so much better quality CVs are presented in D_2O than that in H_2O solution. As shown in Fig. 6, a broad oxidative peak appears in the positive-going sweep and a reductive peak appears in the reverse sweep. With the increase of the number of the cyclic scan, the current of redox peaks continually decrease in Fig. 6a. The potential of redox peaks shifts positively simultaneously, making the value of ΔE_p unchanged. The phenomenon that redox peaks decrease occurs also with the addition of sodium lactate shown in Fig. 6b. These two results illustrated that the activity of redox of bacteria decreased in deuterated water solution, indicating that D_2O indeed depresses the bacterial metabolism. But the cells still exhibit a weak capability of metabolism and can transfer electrons in a short time.

Moreover, the different effects of cellular toxicity of D_2O on cell proliferation for two strains were also investigated by the cell growth curve, in which $OD_{600\,nm}$ value represents the bacterial population density. Cells were cultured aerobically in LB media prepared with H_2O or D_2O without shaking at 30 °C. From Fig. 7, it can be clearly observed that the growth of wild type and its mutant in water solution underwent four periods, i.e. adaptation period (before 5 h), the logarithmic growth phase (5 h ∼ 33 h), growth stable period and decline phase. A significant growth inhibition of wild type was found in D_2O medium until culturing over 40 h while lower amount mutant was breed. These results showed that D_2O are more significantly harmful to strain with OmcA-MtrC protein knock-out than wild type. It can be also illustrated that OmcA-MtrC protein in the cell outer membrane played an important role of adaptive ability to adverse condition further bearing cellular toxicity. The two strains used in our FTIR / CV experiment were marked in the cell growth curve shown in Fig. 7. Although D_2O toxic effect to cells is different, the cells are alive but strongly inhibited thus the intensity of CV current decrease with the cycles (shown in Fig. 6b). This is the reason why the carbonyl group of 1742 and 1712 cm^{-1} were observed and the intensity of the band at 1742 cm^{-1} is much lower than that in water.

Combined with the results in H_2O and D_2O solution, the band at ca. 1684 cm^{-1} in H_2O solution may be the $\nu_{as(-COO)}$ stretching vibration of carboxyl groups of lactate rather than the water, but seriously affected by the water. It is an important marking of the oxidation of lactate. In addition, we used the electrochemical modulation P- or S-polarized FTIR spectroscopy to distinguish the dissolved species and the surface adsorptive species and the result

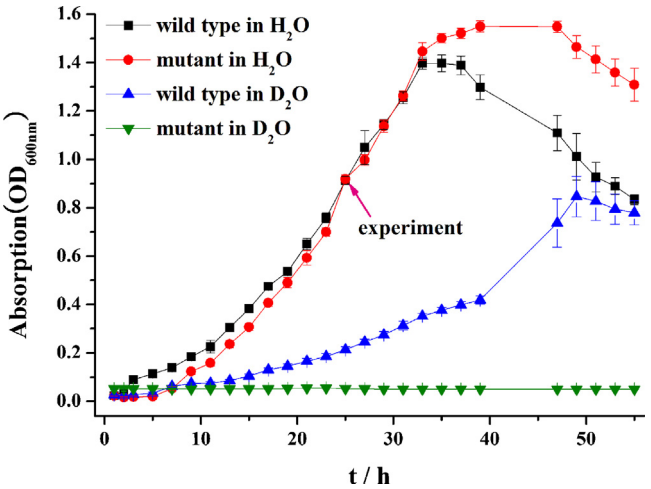

Fig. 7. The cell growth curve of *S. oneidensis* MR-1 wild type and △*omcA*-△*mtrC* mutant cultured in LB medium prepared with H_2O or D_2O.

is shown in ESI Fig. 4. The results indicated that the lactate may be adsorbed through carboxyl to the Au electrode surface in PBS D_2O solution.

Tang et al. reported that *S. oneidensis* has different metabolic pathways: when in the adverse environment, its capability of metabolism weakens, and lactate was transformed to other products rather than CO_2 [36]. Therefore, the capability of metabolism of bacteria can be assessed by determining CO_2 amount, and it also agrees with our viewpoint. This explains why no CO_2 IR band appears in D_2O spectra in Fig. 5, and the difference between Fig. 4 and Fig. 5 would be easily understood.

According to the IR bands change and the species difference, we conclude that the band at 1742 cm^{-1} is attributed to the $\nu_{(C=O)}$ stretching vibration of carboxyl groups in OmcA-MtrC, while 1712 cm^{-1} is related to some unknown transferring-electron protein. When the bacteria suffers from cytotoxicity by D_2O, the outer membrane protein OmcA-MtrC is damaged and inactivated. In this case, other proteins may begin to work and result in the band appearing at 1712 cm^{-1}. This is exactly like what observed in Fig. 5a. OmcA-MtrC will be activated again under the stimulation of substrate, resulting in the band reappearing at 1742 m^{-1} with the addition of lactate (see Fig. 5b and ESI Fig. 5).

4. Conclusions

This work studied the directly extracellular electron transfer of *S. oneidensis* MR-1 wild type and △*omcA*-△*mtrC* mutant. It can be known from cyclic voltammetry, both wild type and mutant have a pair of redox peaks that were ascribed to be a series of proteins (*c*-type cytochromes). Moreover, the wild type and the mutant possess the enhanced capability of electron transfer with addition of lactate.

From electrochemical in situ FTIR results, the capacity of metabolism of the wild type is higher than that of the mutant according to CO_2 measurement; Compared with water and deuterated water, we attribute the band 1742 cm^{-1} and 1712 cm^{-1} to the characteristic groups of OmcA-MtrC and an unknown protein respectively. We thus inferred that OmcA-MtrC protein exhibited the IR band at 1742 cm^{-1}; while the directly EET process of the mutant was carried out by the unknown protein and displayed the IR band at 1712 cm^{-1}. The EET process with OmcA-MtrC protein is much stronger than that with unknown protein.

Although many questions still remain open, electrochemical in situ FTIR is a useful tool to investigate the electron transfer processes as it provides more information at a molecular level. It shed lights on the study of the capability of bacterial metabolism.

Acknowledgement

The authors thank Prof. Kenneth H. Nealson (University of Southern California) for giving *Shewanella oneidensis* MR-1 and its △*omcA*-△*mtrC* mutant. This study was supported by grants from the National Natural Science Foundation of China (Grant Nos. 21321062, 21322703</GN2>, <GN1>21273180) and State Key Laboratory of Supramolecular Structure and Materials of Jilin University (SKLSSM201440).

Appendix A. Supplementary data

Supplementary data associated with this article can be found, in the online version, at http://dx.doi.org/10.1016/j.electacta. 2015.04.139.

References

[1] C.R. Myer, K.H. Nealson, Bacterial manganese reduction and growth with manganese oxide as the sole electron acceptor, Science 240 (4857) (1988) 1319–1321.
[2] I. Sokolov, D.S. Smith, G.S. Henderson, Y.A. Gorby, F.G. Ferris, Cell surface electrochemical heterogeneity of the Fe(III)-reducing bacteria Shewanella putrefaciens, Environment and Science Technology 35 (2) (2001) 341–347.
[3] J.M. Myers, C.R. Myers, Role for outer membrane cytochromes OmcA and OmcB of Shewanella putrefaciens MR-1 in reduction of manganese dioxide, Applied and environmental microbiology 67 (1) (2001) 260–269.
[4] (a) B. Shi, Z. Chen, D.A. Wang, M.U. Elias, Y.A. Mayer, S. Gorby, B.H. Ni, D.W. Lower, D.S. Kennedy, H.M. Wunschel, M.J. Mottaz, E.A. Marshall, A.S. Hill, J.M. Beliaev, J.K. Zachara, T.C. Squier Fredrickson, Isolation of a high-affinity functional protein complex between OmcA and MtrC: two outer membrane decaheme c-Type cytochromes of Shewanella oneidensis MR-1, Journal of Bacteriology 188 (13) (2006) 4705–4714;
(b) A.C. Mitchell, L. Peterson, C.L. Reardon, S.B. Reed, D.E. Culley, M.R. Romine, G.G. Geesey, Role of outer membrane c-type cytochromes MtrC and OmcA in Shewanella oneidensis MR-1 cell production, accumulation, and detachment during respiration on hematite, Geobiology 10 (4) (2012) 355–370.
[5] R.A. Bouhenni, G.J. Vora, J.C. Biffinger, S. Shirodkar, K. Brockman, R. Ray, P. Wu, B.J. Johnson, E.M. Biddle, M.J. Marshall, L.A. Fitzgerald, B.J. Little, J.K. Fredrickson, A.S. Beliaev, B.R. Ringeisen, D.A. Saffarini, The role of Shewanella oneidensis MR-1 outer surface structures in extracellular electron transfer, Electroanalysis 22 (7–8) (2010) 856–864.
[6] L. Shi, K.M. Rosso, T.A. Clarke, D.J. Richardson, J.M. Zachara, J.K. Fredrickson, Molecular underpinnings of Fe(III) oxide reduction by Shewanella oneidensis MR-1, Frontiers in Microbiology 3 (2012) 50.
[7] G.F. White, Z. Shi, L. Shi, Z.M. Wang, A.C. Dohnalkova, M.J. Marshall, J.K. Fredrickson, J.M. Zachara, J.N. Butt, D.J. Richardson, T.A. Clarke, Rapid electron exchange between surface-exposed bacterial cytochromes and Fe(III) minerals, Proceedings of the National Academy of Sciences of the United States of America 110 (16) (2013) 6346–6351.
[8] A.A. Carmona-Martinez, F. Harnisch, L.A. Fitzgerald, J.C. Biffinger, B.R. Ringeisen, U. Schroder, Cyclic voltammetric analysis of the electron transfer of Shewanella oneidensis MR-1 and nanofilament and cytochrome knock-out mutants, Bioelectrochemistry 81 (2) (2011) 74–80.
[9] E. Marsili, D.B. Baron, I.D. Shikhare, D. Coursolle, J.A. Gralnick, D.R. Bond, Shewanella secretes flavins that mediate extracellular electron transfer, Proceedings of the National Academy of Sciences 105 (10) (2008) 3968–3973.
[10] A. Okamoto, K. Hashimoto, K.H. Nealson, R. Nakamura, Rate enhancement of bacterial extracellular electron transport involves bound flavin semiquinones, Proceedings of the National Academy of Sciences of the United States of America 110 (19) (2013) 7856–7861.
[11] (a) A.S. Beliaev, D.A. Saffarini, J.L. McLaughlin, D. Hunnicutt, MtrC, an outer membrane decahaem c cytochrome required for metal reduction in Shewanella putrefaciens MR-1, Molecular Microbiology 39 (3) (2001) 722–730;
(b) C.R. Myers, J.M. Myers, Cell surface exposure of the outer membrane cytochromes of Shewanella oneidensis MR -1, Letters in Applied Microbiology 37 (2003) 254–258.
[12] M.E. Hernandez, D.K. Newman, Extracellular electron transfer, Cellular and Molecular Life Sciences 58 (2001) 1562–1571.
[13] G. Reguera, K.D. McCarthy, T. Mehta, J.S. Nicoll, M.T. Tuominen, T.D. Lovley, Extracellular electron transfer via microbial nanowires, Nature Letter 435 (23) (2005) 1098–1101.
[14] Y.A. Gorby, S. Yanina, J.S. McLean, K.M. Rosso, D. Moyles, A. Dohnallkova, T.J. Beveridge, I.S. Chang, B.H. Kim, K.S. Kim, D.E. Culley, S.B. Reed, M.F. Romine, D. A. Saffarini, E.A. Hill, L. Shi, D.A. Elias, D.W. Kennedy, G. Pinchuk, K. Watanabe, S. Ishii, B. Logan, K.H. Nealson, J.K. Fredrickson, Electrically conductive bacterial nanowires produced by Shewanella oneidensis strain MR-1 and other microorganisms, Proceedings of the National Academy of Sciences 103 (30) (2006) 11358–11363.
[15] K. Fricke, F. Harnisch, U. Schroder, On the use of cyclic voltammetry for the study of anodic electron transfer in microbial fuel cells, Energy and Environmental Science 1 (2008) 144–147.
[16] L.A. Meitl, C.M. Eggleston, P.J.S. Colberg, N. Khare, C.L. Reardon, L. Shi, Electrochemical interaction of Shewanella oneidensis MR-1 and its outer membrane cytochromes OmcA and MtrC with hematite electrodes, Geochimica et Cosmochimica Acta 73 (18) (2009) 5292–5307.
[17] A. Okamoto, R. Nakamura, K. Hashimoto, In-vivo identification of direct electron transfer from Shewanella oneidensis MR-1 to electrodes via outer-membrane OmcA–MtrCAB protein complexes, Electrochimica Acta 56 (16) (2011) 5526–5531.
[18] D. Baron, E. LaBelle, D. Coursolle, J.A. Gralnick, D.R. Bond, Electrochemical measurement of electron transfer kinetics by Shewanella oneidensis MR-1, Journal of biological chemistry 284 (2009) 28865–28873.
[19] W. Jiang, A. Saxena, B. Song, B.B. Ward, T.J. Beveridge, S.C.B. Myneni, Elucidation of functional groups on gram-positive and gram-negative bacterial surfaces using infrared spectroscopy, Langmuir 20 (26) (2004) 11435–11442.
[20] S.J. Parikh, J. Chorover, ATR-FTIR spectroscopy reveals bond formation during bacterial adhesion to Iron oxide, Langmuir 22 (20) (2006) 8492–8500.

[21] J.J. Ojeda, M.E. Romero-Gonzalez, R.T. Bachmann, R.G.J. Edyvean, S.A. Banwart, Characterization of the cell surface and cell wall chemistry of drinking water bacteria by combining XPS, FTIR spectroscopy, modeling, and potentiometric titrations, Langmuir 24 (8) (2008) 4032–4040.
[22] E.J. Elzinga, J.H. Huang, J. Chorover, R. Kretzschmar, ATR-FTIR spectroscopy study of the influence of pH and contact time on the adhesion of Shewanella putrefaciens bacterial cells to the surface of hematite, Environment and Science Technology 46 (23) (2012) 12848–12855.
[23] J.P. Busalmen, A.E. Nunez, A. Berna, J.M. Feliu, C-Type cytochromes wire electricity-producing bacteria to electrodes, Angewandte Chemie 120 (26) (2008) 4952–4955.
[24] J.P. Busalmen, A.E. Nunez, A. Berna, J.M. Feliu, ATR-SEIRAs characterization of surface redox processes in G. Sulfurreducens, Bioelectrochemistry 78 (1) (2010) 25–29.
[25] A. Kuzumea, U. Zhumaeva, J.F. Li, Y.C. Fu, M. Füeg, A. Esteve-Nunez, T. Wandlowski, An in-situ surface electrochemistry approach toward whole-cell studies: Charge transfer between Geobacter sulfurreducens and electrified metal/electrolyte interfaces through linker molecules, Electrochimica Acta 112 (2013) 933–942.
[26] B.E. Logan, K. Rabaey, Conversion of Wastes into Bioelectricity and Chemicals by Using, Science 337 (2012) 686–690.
[27] D.R. Lovley, Electromicrobiology, Annual Review of Microbiology 66 (2012) 391–409.
[28] (a) T.E. Meyer, I. Tsapin, D. Smet, K.H. Nealson, M.A. Cusanovich, J.J. van Beeumen, Identification of 42 possible cytochrome c genes in the Shewanella oneidensis genome and characterization of six soluble cytochromes, OMICS 8 (2004) 57–77;
(b) O. Bretschger, A. Obraztsova, C.A. Sturm, S.C. In, Y.A. Gorby, S.B. Reed, D.E. Culley, C.L. Reardon, S. Barua, M.F. Romine, J. Zhou, A.S. Beliaev, R. Bouhenni, D. Saffarini, F. Mansfeld, B.H.J.K. Kim Fredrickson, K.H. Nealson, Applied and Environmental, Microbiology 73 (2007) 7003–7012;
(c) R.R. Wu, L. Cui, L.X. Chen, C. Wang, C.L.G.P. Cao Sheng, H.Q. Yu, F. Zhao, Effects of Bio-Au Nanoparticles on Electrochemical activity of Shewanella oneidensis wild type and △omcA/mtrC mutant, Scientific Reports 3 (2013) 3307.
[29] R. Woods In Electroanalytical Chemistry. A Series of Advances; A. J. Bard, Eds. ; D. Marcel, Inc. : New York, Basel, 1976; Vol. 9, p. 24-27.
[30] S.G. Sun, D.F. Yang, Z.W. Tian, In situ FTIR studies on the adsorption and oxidation of n-propanol and isopropanol at a platinum electrode in sulphuric acid solutions, Journal of Electroanalytical chemistry 289 (1-2) (1990) 177–187.
[31] L.X. You, Y.M. Fang, J.W. Guo, L. Zhang, J.S. Chen, J.J. Sun, Mechanism of electro-catalytic oxidation of shikimic acid on Cu electrode based on in situ FTIRS and theoretical calculations, Electrochimica Acta 112 (58) (2011) 165–171.
[32] U. Oesch, J. Janata, Electrochemical study of gold electrodes with anodic oxide films-I. formation and reduction behaviour of anodic oxides on gold, Electrochimica Acta 28 (9) (1983) 1237–1246.
[33] (a) F.A. Armstrong, G.S. Wilson, Recent developments in faradaic bioelectrochemistry, Electrochimica Acta 45 (15∼16) (2000) 2623–2645;
(b) Y.Y. Wang, Y.X. Jiang, A. Susha, A. Rogach, S.G. Sun, Effect of pH and Au nanoparticles on cytochrome *c* investigated by electrochemistry and UV-vis absorption spectroscopy, Acta Physico-Chimica Sinica 28 (5) (2012) 1127–1133.
[34] G. Cammas, M. Morssli, E. Fabregue, L. Bardet, Vibrational spectra of lactic acid and lactates, Journal of Raman Spectroscopy 22 (7) (1991) 409–413.
[35] H. Wang, K. Hollywood, R.M. Jarvis, J.R. Lloyd, R. Goodacre, Phenotypic characterization of Shewanella oneidensis MR-1 under aerobic and anaerobic growth conditions by using fourier transform infrared spectroscopy and high-performance liquid chromatography analyses, Applied and Environmental Microbiology 76 (18) (2010) 6266–6276.
[36] Y.J. Tang, J.S. Hwang, D.E. Wemmer, J.D. Keasling, Shewanella oneidensis MR-1 fluxome under various oxygen conditions, Applied and Environmental Microbiology 73 (3) (2007) 718–729.